Determination of Epithelial Na^+ Channel Subunit Stoichiometry from Single-Channel Conductances

Arun Anantharam[1,2] and Lawrence G. Palmer[2]

[1]Graduate Program in Neuroscience and [2]Department of Physiology and Biophysics, Weill Medical College of Cornell University, New York, NY 10021

The epithelial Na^+ channel (ENaC) is a multimeric membrane protein consisting of three subunits, α, β, and γ. The total number of subunits per functional channel complex has been described variously to follow either a tetrameric arrangement of 2α:1β:1γ or a higher-ordered stoichiometry of 3α:3β:3γ. Therefore, while it is clear that all three ENaC subunits are required for full channel activity, the number of the subunits required remains controversial. We used a new approach, based on single-channel measurements in *Xenopus* oocytes to address this issue. Individual mutations that alter single-channel conductance were made in pore-lining residues of ENaC α, β, or γ subunits. Recordings from patches in oocytes expressing a single species, wild type or mutant, of α, β, and γ showed a well-defined current transition amplitude with a single Gaussian distribution. When cRNAs for all three wild-type subunits were mixed with an equimolar amount of a mutant α-subunit (either S589D or S592T), amplitudes corresponding to pure wild-type or mutant conductances could be observed in the same patch, along with a third intermediate amplitude most likely arising from channels with at least one wild-type and at least 1 mutant α-subunit. However, intermediate or hybrid conductances were not observed with coexpression of wild-type and mutant βG529A or γG534E subunits. Our results support a tetrameric arrangement of ENaC subunits where 2α, 1β, and 1γ come together around central pore.

The Journal of General Physiology

INTRODUCTION

The epithelial Na^+ channel mediates the transport of Na^+ across the apical membrane of epithelial cells in a variety of tissues, including the kidney, colon, salivary glands, and lung (Benos and Stanton, 1999; Kellenberger and Schild, 2002; Snyder, 2002). Movement of Na^+ down its electrochemical gradient through these channels underlies fluid homeostasis and control of blood pressure (kidney), salt taste transduction (tongue), and alveolar fluid clearance (lung), and is blocked by submicromolar concentrations of the diuretic amiloride. Instances of aberrant channel activity are associated with several well-characterized physiological diseases. Mutations resulting in increased channel activity lead to hypertension, as in Liddle's syndrome, whereas reduced channel activity is associated with hypotension, as observed in pseudohypoaldosteronism type I (Shimkets et al., 1994; Hansson et al., 1995; Snyder et al., 1995; Schild et al., 1996; Snyder, 2002).

In most epithelia, ENaC consists of three homologous (~30%) α, β, and γ subunits (Canessa et al., 1994). Each subunit is composed of two membrane-spanning regions with cytoplasmic NH_2 and COOH tails, linked by a large extracellular loop that contains several N-glycosylation sites and target residues for proteases that can alter channel activity (Benos and Stanton, 1999; Kellenberger and Schild, 2002; Snyder, 2002). Heterologous expression studies in *Xenopus* oocytes have shown that maximal channel current is detected only when all three subunits α, β, and γ are coexpressed. Expression of the α-subunit alone or with either the β- or γ-subunit results in low but measurable channel activity; expression of the β- and/or γ-subunit does not give rise to detectable channel current (Fyfe and Canessa, 1998). Biophysically, the channel is characterized as being slightly selective for Li^+ over Na^+, and greatly selective for Na^+ over (>100) K^+ (Kellenberger and Schild, 2002). The channel conductance for Na^+ is small (4–5 pS) and channel kinetics are slow and do not show strong voltage dependence (Palmer and Frindt, 1986).

Because the crystal structure for ENaC has not yet been solved, the organization and arrangement of channel subunits must be inferred from functional experiments, usually involving electrophysiology in heterologous expression systems, or from biochemical assays. From these data, it appears that all channel subunits contribute to the Na^+ permeation pathway (Schild et al., 1997; Kellenberger and Schild, 2002). The putative selectivity filter has been localized to a three-residue (G/SxS) track immediately preceding the M2 or second transmembrane region of the ENaC subunits, situated at the narrowest part of the pore excluding all but the smallest cations (Palmer and Andersen, 1989; Schild et al., 1997;

Correspondence to Lawrence G. Palmer: lgpalm@med.cornell.edu

Abbreviations used in this paper: ENaC, epithelial Na^+ channel; wt, wild type.

α-sub	579	G	S	Q	W	S	L	W	F	G	S	**S**	V	L	**S**
β-sub	521	G	G	Q	F	G	F	W	M	**G**	G	S	V	L	C
γ-sub	533	G	**G**	Q	L	G	L	W	M	S	C	S	V	V	C

Figure 1. Sequence alignment of rat α, β, and γ subunits. The number of the start residue in the sequence is indicated. Residues mutated in this study are in bold. The region corresponding to the putative ENaC selectivity filter is shaded in gray.

Kellenberger et al., 1999a,b, 2001). The amiloride binding domain is presumed to be located in the preM2 region of the channel at the outer mouth of the pore (Schild et al., 1997; Kellenberger et al., 2003). Still, our knowledge about many important features of the channel, such as ratiometric arrangement of subunits, is limited.

Previous attempts to investigate the question of subunit stoichiometry have taken various forms. Some groups used measurements of macroscopic current following an approach devised to estimate Shaker K^+ channel stoichiometry (Mackinnon, 1991). Although the methodologies in these instances were similar, the resulting data supported both a 2α:1β:1γ (Firsov et al., 1998; Kosari et al., 1998) and a 3α:3β:3γ stoichiometry (Snyder et al., 1998). Biochemical studies involving sucrose density sedimentation have likewise yielded conflicting results (Snyder et al., 1998; Dijkink et al., 2002). Results from freeze-fracture electron microscopy experiments supported a higher order arrangement of subunits (Eskandari et al., 1999) as did data from studies using FRET and FIR (Staruschenko et al., 2004, 2005). However, functional studies using concatamers where subunits were linked head to tail in a fixed ratio showed that a 2α:1β:1γ organization most closely resembles the biophysical properties of the heteromer both at the macroscopic and single-channel level (Firsov et al., 1998).

The purpose of this study was to determine the subunit stoichiometry of the epithelial Na^+ channel from single-channel conductances. The methodology follows that of several previous studies (Veatch and Stryer, 1977; Durkin et al., 1990; Cooper et al., 1991; Liu et al., 1996; Premkumar and Auerbach, 1997; Li et al., 2006). Mutations were made in residues lining the ionic permeation pathway such that single-channel conductance for Na^+ and Li^+ were altered. Subsequently, the event amplitudes of single channels formed by purely mutant, wt, or a mixture of mutant and wt subunits in *Xenopus* oocytes were measured and analyzed. Our data provide support for a model where 2α, 1β, and 1γ subunits come together around a central pore.

MATERIALS AND METHODS

Site-directed Mutagenesis and Channel Expression

Site-directed mutagenesis was performed on rat α, β, or γ ENaC cDNA using the QuikChange kit from Stratagene following the manufacturer's instructions. To confirm that the mutations were successful, cDNAs were sent to the Cornell University Bio Resource Center for sequencing (Ithaca, New York). Plasmids containing rat ENaC α, β, and γ subunits were linearized with the Not I restriction enzyme (New England Biolabs) and cRNAs were synthesized in vitro using the mMESSAGE mMACHINE kit (Ambion) as previously described (Anantharam et al., 2006). Stage V–VI oocytes were harvested from *Xenopus laevis* and defolliculated by incubating in an OR2 solution containing 2 mg/ml collagenase type II (Worthington) and 2 mg/ml hyaluronidase type II (Sigma-Aldrich) left gently shaking for 60 min at room temperature. Healthy oocytes were selected and pressure injected with 100 nl of a solution containing 80 ng/μl of wt and/or mutant α, β, and γ subunits. During the expression phase, the oocytes were kept in modified Barth's saline (MBS), pH 7.4 containing (in mM) 1 NaCl, 40 KCl, 60 NMDG, 0.7 $CaCl_2$, 0.8 $MgSO_4$, and 5 HEPES. All chemicals were from Sigma-Aldrich unless otherwise noted.

Electrophysiology

Two Electrode Voltage Clamp (TEVC). Oocytes were bathed in a standard extracellular recording solution containing (in mM) 110 NaCl, 2 $CaCl_2$, 1 $MgCl_2$, 2 KCl, 5 HEPES, pH 7.4. For selectivity experiments, Na^+ was replaced by Li^+ at the same concentration. Whole cell currents were measured in intact oocytes using a two-electrode voltage clamp (OC-725; Warner Instrument Corp.) with ITC-16 interface (Instrutech) running Pulse software (Heka Elektronik). Pipets were fabricated using hematocrit capillary tubes (Fisher Scientific) with a three-step vertical pipet puller (Kopf). The resistance of the pipets was 0.5–1 MΩ, when filled with 3 M KCl. Steady-state current–voltage curves were generated from a step-voltage protocol consisting of 15 pulses lasting 50 ms from −100 to +40 mV, from a holding potential of 0 mV. Measurements of I_{Na}, the amiloride-sensitive current (difference between Na^+ currents obtained in the presence of 100 μM amiloride from those obtained in the absence of amiloride at −100 mV) were made 16–24 h after injection. Due to the higher K_i of the $\alpha\beta$G529Aγ channel for amiloride, 250 μM amiloride was used in this instance (Kellenberger et al., 1999b).

Patch Clamp. Prior to patching the oocyte, the vitelline membrane was mechanically removed in a hypertonic K^+ bath solution (to depolarize the membrane) containing 200 mM sucrose. The bath solution contained (in mM) 110 KCl, 2 $CaCl_2$, 1 $MgCl_2$, 5 HEPES, pH 7.4. The pipet solution contained (in mM) 110 LiCl or NaCl, 1 $MgCl_2$, and 5 HEPES, at pH 7.4. Patch-clamp pipets were prepared from hematocrit capillary glass (Fisher Scientific) using a vertical puller (Kopf Instruments) and fire polished with a microforge to yield resistances of 3–8 MΩ. Currents from patches containing channels were recorded with an EPC-7 patch-clamp amplifier (Heka Elektronik) for a duration of 1–10 min, and digitized with a Digidata 1332A interface (Axon Instruments). Data were sampled at 1 kHz and analyzed with pCLAMP9 software (Axon Instruments). For analysis, single-channel recordings were filtered using a lowpass Bessel filter at 40 Hz. All-points and event-amplitude histograms were constructed using computer routines in Clampfit. Event amplitudes were measured by fitting the individual channel openings with idealized square waves using the built-in event detection function. Only openings that reached a plateau were used and openings shorter than 10 ms were discarded. Histograms were fit by Gaussian functions using a curve-fitting routine, also in Clampfit.

The two-tailed Student's *t* test was used to determine whether differences between groups were significant (with Microcal Origin 6.0 software). Data are presented as means ± SEM or means ± standard deviation, as indicated.

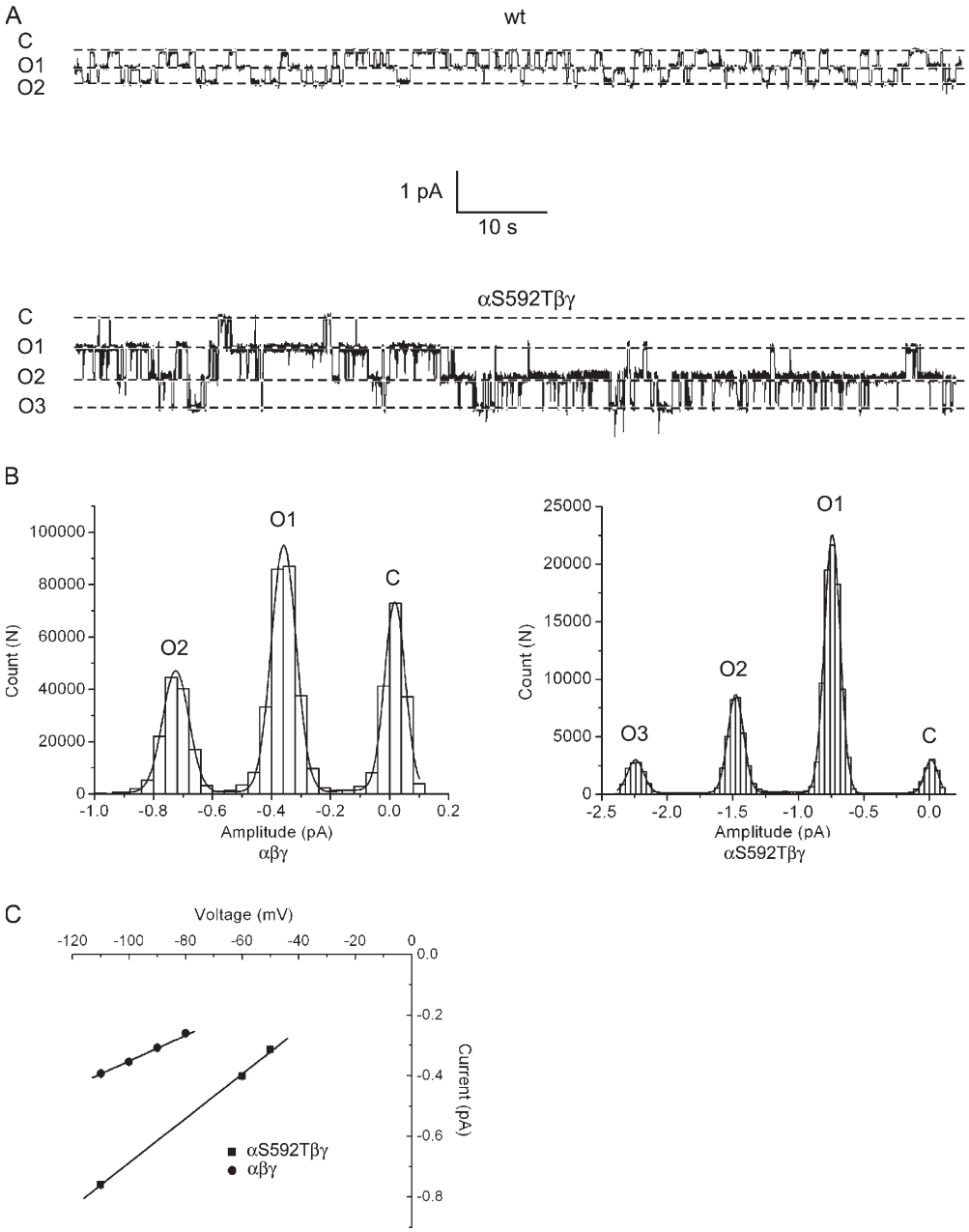

Figure 2. Single-channel properties of αβγ (wt) and αS592Tβγ channels with Na^+ as the charge carrier. Cell-attached patch recordings were taken from oocytes expressing either wt-α or αS592T together with wt β and γ. (A) Exemplar traces of 100 s duration from patches containing wt or αS592Tβγ channels in the patch, with Na^+ as the charge carrier. The pipet voltage was +110 mV. Downward deflections show inward current from the pipet to the cell from a fully closed (C) level to a number of open levels (O) as indicated. (B) All-points histograms were constructed from brief regions of the single-channel recordings obtained in A. The histograms were fit by either three (wt) or four (mutant) Gaussian functions corresponding to closed and open levels. Open conductance levels were of a single amplitude and no subconductances were observed. (C) Slope conductances of wt and αS592Tβγ channels were obtained from single-channel i-V relationships as shown. Conductance was calculated to be 4.2 ± 0.2 pS for the wt channel and 7.2 ± 0.2 pS for the mutant channel.

RESULTS

To investigate the subunit stoichiometry of ENaC we used a method based on single-channel conductances. Wild-type (wt) channels and channels harboring a mutation in a single subunit were expressed separately in oocytes. Single-channel events were monitored by patch clamp and binned by size to construct either transition-amplitude or all-points histograms. Next, mixtures of wt and mutant subunits were coexpressed in oocytes at an equimolar ratio and the process repeated. The existence of hybrid channels was inferred from the appearance of event amplitudes intermediate to those corresponding to wt or mutant channels. Potential mutations for use in this study (Fig. 1) were identified by a literature search and pursued if (a) the mutant channel showed a unique conductance level for the permeant ion of interest (Na^+ or Li^+), and (b) the difference between wt and mutant conductances was large enough that conductances of an intermediate size could be distinguished by our detection method.

α-Subunit (S592T)

A serine residue was changed to threonine (S→T) in the α-subunit of ENaC at position 592. This channel, which we call αS592Tβγ, was first characterized by Waldmann and colleagues, in a study where amino acid residues in the TM2 region of ENaC were systematically replaced with their corresponding residues from the *Caenorhabditis*

TABLE I

Macroscopic and Single-Channel Properties of Wild-Type and Mutant Epithelial Na^+ Channels

Channel	I_{Na} (μA)	I_{Li}/I_{Na}	G_{Li}/G_{Na}	P_{Li}/P_{Na}	g_{Na} (pS)	g_{Li} (pS)
Wild-type	−2.7 ± 0.4	3.3 ± 0.3	3.5 ± 0.2	2.3 ± 0.4	4.2 ± 0.2	7.0 ± 0.1[d]
αS589D	−1.3 ± 0.4[a]	2.3 ± 0.2[a]	2.7 ± 0.3[a]	0.6 ± 0.1[b]	ND	1.9 ± 0.1
αS592T	−19.2 ± 3.0[c]	1.1 ± 0.1[c]	1.2 ± 0.1[c]	0.7 ± 0.1[b]	7.2 ± 0.2	ND
βG529A	−1.1 ± 0.2[a]	0.3 ± 0.07[c]	0.3 ± 0.1[c]	0.2 ± 0.1[c]	ND	1.9 ± 0.3
γG534E	−4.8 ± 1.3	1.3 ± 0.4[b]	1.4 ± 0.1[b]	0.8 ± 0.1[b]	ND	6.7 ± 0.1[e]

Whole-cell (n = 5–8) and single-channel (n = 2–5) properties of wt and mutant channels were studied in oocytes. Mutant channels are listed by mutated subunit only, although all three subunits were always expressed. I, macroscopic current; G, macroscopic conductance; P_{Li}/P_{Na}, permeability ratio of Li^+ to Na^+; g, single-channel conductance; ND, not determined. Data presented as mean ± SEM.

[a]Statistically significant compared to wt channel; $P < 0.05$.

[b]$P < 0.005$, compared to wt.

[c]$P < 0.0005$, compared to wt.

[d]Wild-type channel g_{Li} with 2 mM Ca^{2+} in pipet = 5.5 ± 0.2 pS.

[e]Mutant γG534E channel g_{Li} with 2 mM Ca^{2+} in pipet = 3.4 ± 0.1 pS.

elegans protein Mec-4 (Waldmann et al., 1995). The channel was reported to have a g_{Na} that was roughly twofold higher than that of the wt channel while most of its other biophysical properties remained unchanged.

In order for our method to succeed, it was first necessary to establish that neither wt rat ENaC nor the mutants used for analysis showed subconductance levels as this could complicate the effort to identify hybrid conductances. We therefore obtained several (n = 5) cell-attached patch recordings (of at least 1 min in duration) from oocytes in which wt channels were expressed, and constructed all-points histograms as shown in Fig. 2 A. The histograms were fit by Gaussian functions corresponding to single open and closed states as depicted. All-points histograms were also constructed from long recordings taken from oocytes expressing mutant αS592Tβγ channels (n = 3) and were again fit with Gaussians corresponding to single closed and open states (Fig. 2 B). The slope conductance for Na^+ was calculated to be ∼4.2 pS for the wt channel and 7.2 pS for the mutant channel (Fig. 2 C; see also Table I), similar to previously reported values (Waldmann et al., 1995).

The difference in current–transition amplitudes between wt and mutant ENaC (∼0.3 pA) appeared large enough that the presence of intermediate current levels could be reasonably detected by our method. To determine if this was true, we mixed α-wt and αS592T subunits at a 1:1 molar ratio along with wt β and γ subunits and coinjected them in oocytes. Channels at the membrane could then be formed by purely wt subunits (α+βγ), mutant αS592T along with wt β and γ subunits (αS592T+βγ), or combination of wt and mutant α subunits along with wt β and γ (αS592T+α+βγ).

In Fig. 3 A we show a 60-s segment of a longer recording where mutant and wt ENaC subunits were expressed in the same oocytes. This particular patch contains channels corresponding to at least three different conductances: a small wt conductance, a larger mutant conductance, and an additional intermediate conductance (marked with stars), not observed in cells where wt channels or mutant channels were expressed alone. In fact, in two out of four recordings taken from oocytes in which wt and mutant subunits were coexpressed, these intermediate events were observed (Table II). To more precisely quantify the conductance level to which the intermediate single-channel events belonged, a cumulative amplitude histogram was constructed as shown in Fig. 3 B. This histogram was best fit by the sum of three Gaussian functions with means of approximately −0.86, −0.73, and −0.54 pA. The simplest interpretation of this result is that the distinct intermediate Gaussian belongs to a hybrid channel, supporting the idea that more than one α-subunit contributes to the ion permeation pathway.

β-Subunit (G529A)

We next searched for mutations in the β-subunit that altered ENaC conductance for Na^+ or Li^+ ions. In a previous study, a G→A mutation in TM2 of the β-subunit at residue 529 was reported to reduce channel Li^+ conductance three- to fourfold (Kellenberger et al., 1999b). To determine whether this mutation would be suitable for our study, we pursued an approach similar to that taken for the α-subunit. First, we confirmed by patch clamp that neither wt nor αβG529Aγ channels exhibited subconductance levels (Fig. 4 A). Recordings (n = 3 wt; n = 2 mutant) were then used to construct all-points histograms that were fit by three Gaussian functions, for a single closed level and two open levels with no subconductances (Fig. 4 B). The slope conductance of the αβG529Aγ channel was determined to be ∼1.9 pS compared with 7.0 pS for the wt channel (Fig. 4 C). Next, wt and mutant β subunits were mixed at a 1:1 ratio and coinjected with wt α and γ subunits into oocytes. The following day, cell-attached patch recordings from oocytes expressing Na^+ channels were obtained. In one case, a recording from an oocyte injected with a mixed pool of subunits showed only a wt (7.0 pS) conductance in the patch. In other cases, both wt and mutant

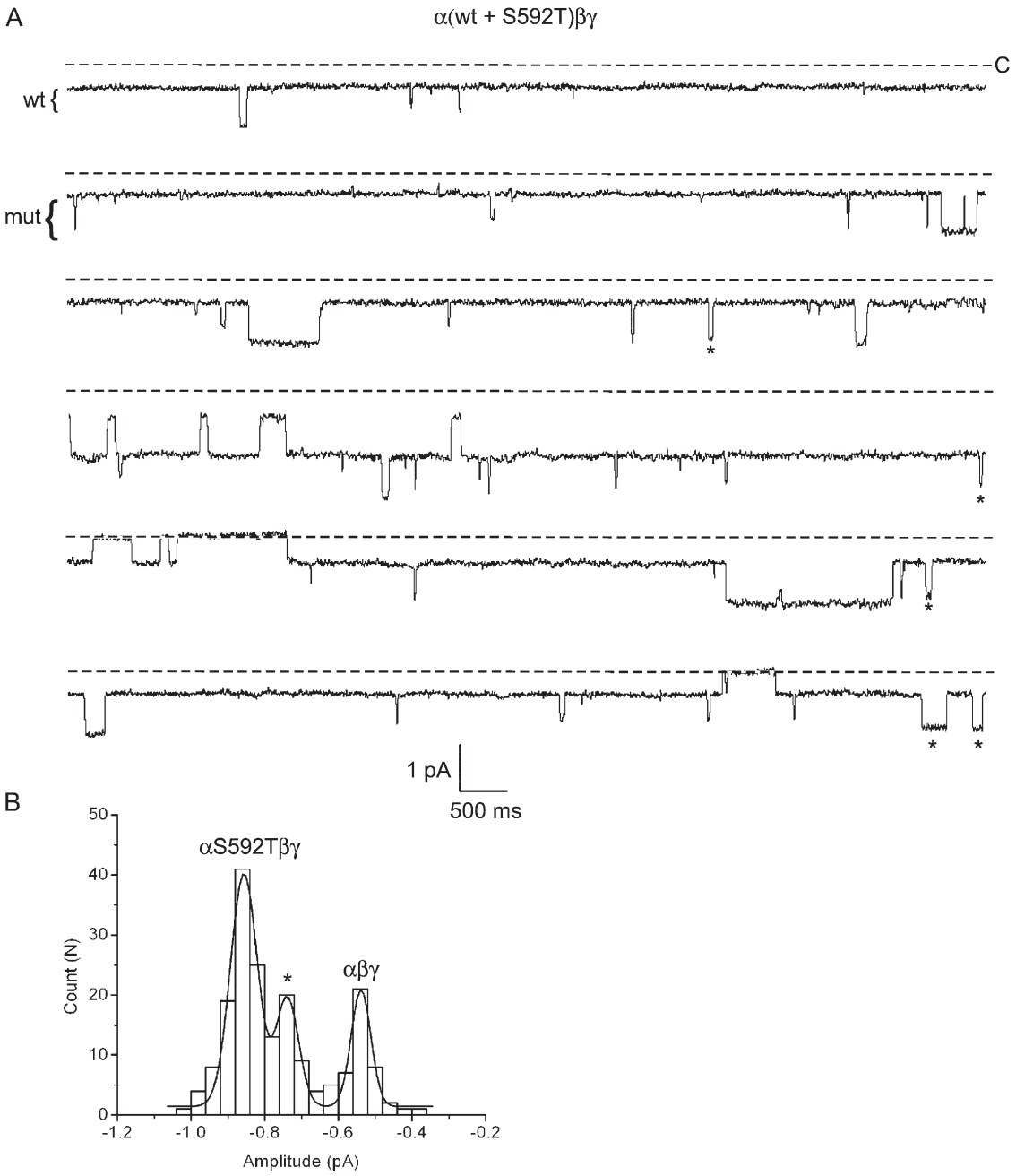

Figure 3. Coexpression of wt and mutant αS592T subunits. Oocytes were injected with α-wt and αS592T subunits, together with wt β and γ. (A) Six sequential 10-s segments of recording from a patch containing wt, mutant, and hybrid channels are shown. The pipet contained Na^+ and the pipet voltage was +110 mV. The wt and mutant conductance levels are indicated by the brackets to the left of the trace. Openings that correspond to a hybrid conductance are marked by a star. (B) An event-amplitude histogram was constructed by measuring the size of every closed to open transition (described in Materials and Methods) from the entire recording in A. The histogram was fit by three Gaussian functions where the parameters were (mean ± SD): −0.54 ± 0.03, −0.86 ± 0.04, and −0.73 ± 0.03 pA (marked by star), for the wt, mutant, and hybrid conductances, respectively.

conductances were observed in the same patch ($n = 6$). An 80-s segment of a recording containing both wt and mutant conductances is shown in Fig. 5 A. For every recording, the sizes of the current level transitions were measured and used to construct an amplitude histogram. The histogram with the largest number of events is shown in Fig. 5 B. The data were fit by two Gaussian functions with means of approximately −0.3 and −0.8 pA, corresponding to event amplitudes of mutant and wt conductances, respectively. Intermediate events were never observed, suggesting that functional epithelial Na^+ channels only require one β-subunit.

If mutant and wt channels associate randomly and express equally well (to a first approximation, this

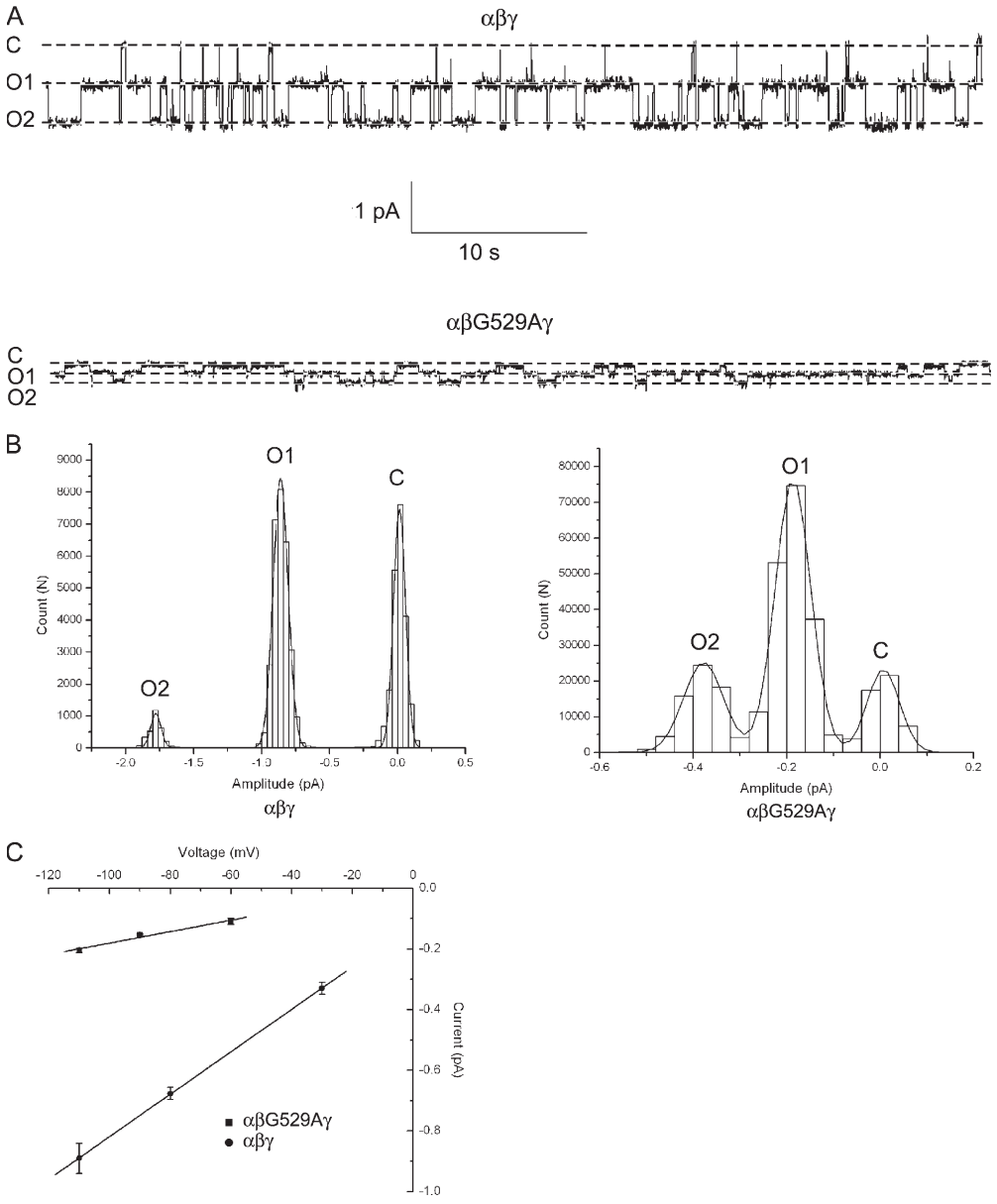

Figure 4. Single-channel properties of wt and αβG529Aγ channels with Li^+ as the charge carrier. Cell-attached patch recordings were taken from oocytes expressing either wt or αβG529Aγ channels. (A) Exemplar single-channel traces of 60 s duration from patches containing wt or αβG529Aγ ENaC with LiCl in the pipet. The pipet voltage was +110 mV. Downward deflections correspond to movement of Li^+ from the pipet to the cell from a fully closed (C) level to two open levels (O) as indicated. (B) All-points histograms were constructed from an ~10-s region of the single-channel recordings obtained in A. The histograms were fit by three Gaussian functions corresponding to closed, one open, and two open levels. No subconductances were observed. (C) Slope conductances of wt and αβG529Aγ channels were obtained from single-channel i-V relationships as shown. Conductance was calculated to be 7.0 ± 0.1 pS for the wt channel and 1.9 ± 0.3 pS for the mutant channel.

assumption seems reasonable as the number of distinct mutant conductances and wt conductances observed in seven recordings were 15 and 21, respectively) in oocytes, then subunit assembly should follow a binomial distribution. If there are two β subunits per channel complex, then the probability of seeing a hybrid occurring is 0.5. The binomial distribution would predict that if x current level transitions or conductances were observed, then the probability of not seeing a single hybrid conductance would equal 0.5^x. Given that ~36 distinct current level transitions were actually observed in 7 recordings, it is very unlikely that should there be two β subunits/complex, an intermediate event corresponding to a hybrid conductance would not occur (0.5^{36} or 1.5×10^{-11}) on statistical grounds. It is even less likely that intermediate events would not occur if one assumes there are three or more β subunits/complex. Thus, it seems reasonable to conclude from our recordings that there is only a single β-subunit in a functional channel.

γ-Subunit (G534E)

In the absence of a structural map for how different ENaC subunits are arranged, it is helpful to make mutations at homologous residues so each affects channel function in a similar way. Mutations at homologous residues in the permeation pathway (TM2) of ENaC (αS581D, βG522D, and γG534E), were shown to decrease g_{Na} and g_{Li} in a Ca^{2+}-dependent manner (Schild et al., 1997). The advantages of using these particular mutations are that (a) their effects on ion conductance are through electrostatics and should therefore

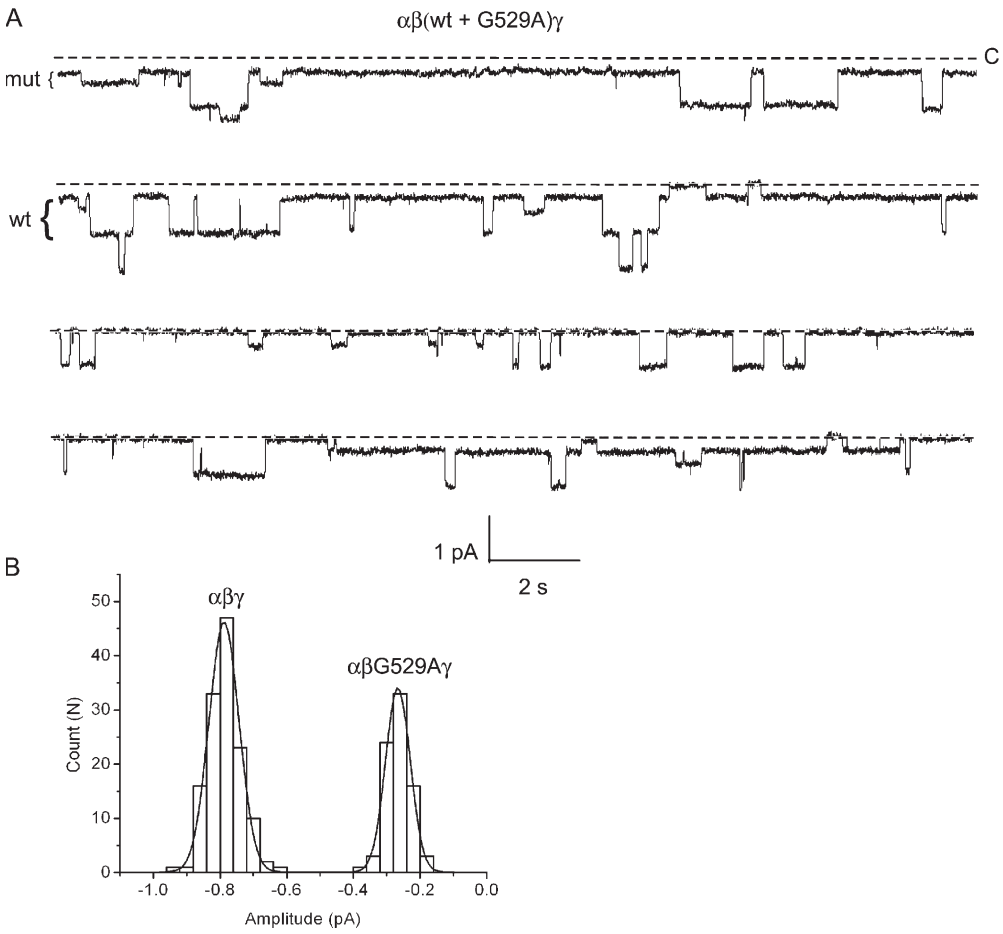

Figure 5. Coexpression of wt and mutant βG529A subunits. Oocytes were coinjected with β-wt and βG529A subunits, together with wt α and γ. (A) An 80-s segment of recording taken from a patch containing wt and mutant channels is shown. The pipet contained Li^+ and the pipet voltage was +110 mV. The amplitude of wt and mutant conductance levels are indicated by brackets to the left of the trace. (B) An event-amplitude histogram was constructed by measuring the size of every closed to open transition for the recording with the most events shown in A (bottom trace). The histogram was fit by two Gaussian functions with parameters (mean ± SD): 0.28 ± 0.04 and 0.79 ± 0.05 pA, corresponding to mutant and wt conductance levels, respectively. Analysis of six other recordings gave similar results.

be additive, and (b) the degree to which conductance is reduced can be titrated to the concentration of extracellular Ca^{2+}. However, of the three mutants tried in our experiments, only the αβγG534E channel showed expression levels in oocytes large enough to pursue single-channel recordings.

Two-electrode voltage clamping (TEVC) of oocytes expressing αβγG534E channels was used to construct a dose–response for Ca^{2+} block. Whereas wt channels were only mildly sensitive to inhibition by external Ca^{2+}, mutant channels were blocked with a K_i of ~1 mM and maximal inhibition of 50% (Fig. 6 A). At a concentration of 2 mM Ca^{2+}, macroscopic current of αβγG534E channels was inhibited by ~40% with either Na^+ or Li^+ in the external bath solution (Fig. 6 B). Wild-type channel unitary currents in the presence of 2 mM Ca^{2+} in the pipet solution were slightly reduced as compared with when Ca^{2+} was absent; moreover, the inclusion of Ca^{2+} in the patch pipet did not result in the appearance of subconductance levels ($n = 2$; Fig. 7 A). On the other hand, inclusion of Ca^{2+} in the pipet solution when recording from channels harboring the γG534E mutation reduced current amplitude by ~40%, mirroring the effect observed at the macroscopic level (Fig. 7 B). No subconductance levels were observed for the mutant channel whether or not Ca^{2+} was in the pipet ($n = 2$ without Ca^{2+}; $n = 3$ with Ca^{2+}). The conductance of the mutant channel for Li^+ was also reduced significantly from 6.7 to 3.4 pS with Ca^{2+} (Fig. 7 D) while the conductance of the wt channel declined only slightly from 7.0 to 5.5 pS (Fig. 7 C).

We next mixed wt and mutant γ subunits together with wt α and β subunits in an effort to discern whether events of an amplitude intermediate to wt channel and mutant channel events could be detected in the presence of Ca^{2+}. Three recordings containing both wt and mutant conductances were obtained. An 80-s segment of one such record is shown in Fig. 8 A. In this instance, current level transitions corresponding to the wt (5.5 pS) and mutant channel (3.4 pS) conductance are clearly evident in the recording. Patches containing only mutant ($n = 2$) or wt channels ($n = 2$) were also obtained, but are not shown. An amplitude histogram was constructed from the recording with the largest number of events and is shown in Fig. 8 B. In a total of seven recordings, current level transitions belonging to a hybrid conductance were never observed. Following the logic explicated for the β-subunit mutant, if there are two γ subunits in a complex, and if channel subunits express equally well (of roughly 26 distinct conductances

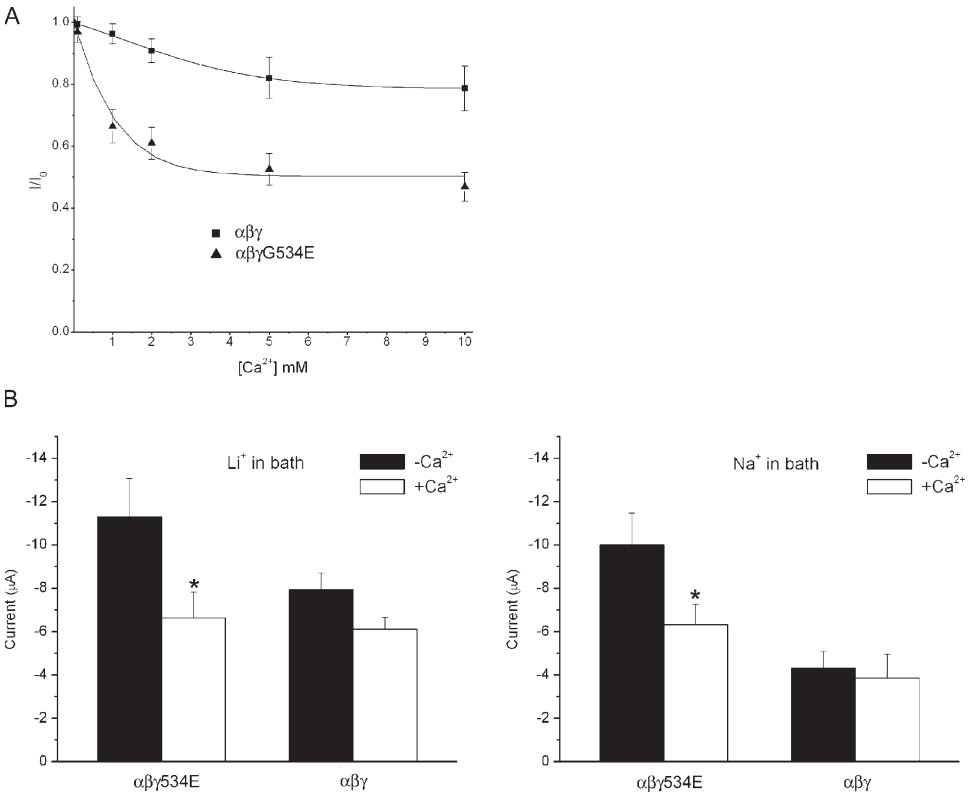

Figure 6. Macroscopic current in oocytes expressing αβγG534E channels is inhibited by Ca^{2+}. (A) Two-electrode voltage clamp was used to generate a dose–response curve showing the effects of increasing $[Ca^{2+}]_{ex}$ on I_{Li} in wt and αβγG534E channels. 100 μM amiloride was applied at the end of each recording to correct for amiloride-insensitive current. (B) Current is inhibited to a similar extent by 2 mM Ca^{2+} whether Li^+ or Na^+ is in the extracellular solution. *, statistically significant compared with current (I_{Li} or I_{Na}) in the absence of Ca^{2+} ($P < 0.05$). Data presented as mean ± SEM for 7–12 oocytes.

observed when wt and mutant subunits were coexpressed in oocytes, 11 belonged to mutant channels and 15 to wt channels) and associate randomly with each other, the probability a hybrid conductance is not observed is exceedingly small (0.5^{26} or 1.5×10^{-8}). From these data, it is unlikely that more than one γ-subunit contributes to functional channel formation.

α-Subunit (αS589D)

We revisited the question of the α-subunit number by using a selectivity filter mutant that had been reported to alter unitary conductance of the channel for Li^+ and Na^+ several fold (Kellenberger et al., 2001). This was done for two reasons: (1) to address our concern that channels with a mutation in the selectivity filter, as in the β-subunit, might not associate with wt subunits (the absence of a hybrid conductance would then lead to the spurious conclusion that only one subunit of a particular type is found in a functional channel); and (2) to confirm that hybrid conductances can also be detected with an α-subunit mutant that reduces unitary conductance, as was done for both β and γ subunits.

Mutant αS589Dβγ channels were expressed in oocytes and characterized in the same way as the previous α-, β-, and γ-subunit mutants used in this study. Patches containing one or more channels were obtained as shown in Fig. 9 A ($n = 3$). The mutant channel displays a low open probability with relatively brief open durations. In the segment of the recording shown, at least two channels are evident. An all-points histogram was constructed for this recording and fit by two Gaussian functions for a single open and closed state (Fig. 9 B). The conductance of the αS589Dβγ channel, calculated from the slope of the single-channel i-V relationship, was ~2 pS (Fig. 9 C).

When wt and mutant subunits were coexpressed in oocytes, event amplitudes corresponding to mutant, wt, and hybrid conductances were observed (Fig. 10 A). Hybrid channels were observed in three of six recordings made when a mixed pool wt and mutant subunits were used. Event amplitudes for the recording shown were binned and used to construct an amplitude histogram that was best fit by three Gaussian functions. The Gaussians had means of approximately −0.86, −0.48, and −0.28 pA, corresponding to the wt, hybrid, and mutant conductance levels, respectively (Fig. 10 B). These data confirm that the functional channel complex is composed of at least two α subunits. We did not observe conductances that would be consistent with more than two α subunits/channel, although due to the small number of events we cannot rule this out.

α-Subunit (αS589D/αS592T)

The large difference in the conductances of the αS589Dβγ (1.9 pS) and αS592Tβγ (7.2 pS) channels suggested to us that intermediate events should be readily apparent when these two α mutants are coexpressed in oocytes. Indeed, in one out of three recordings taken

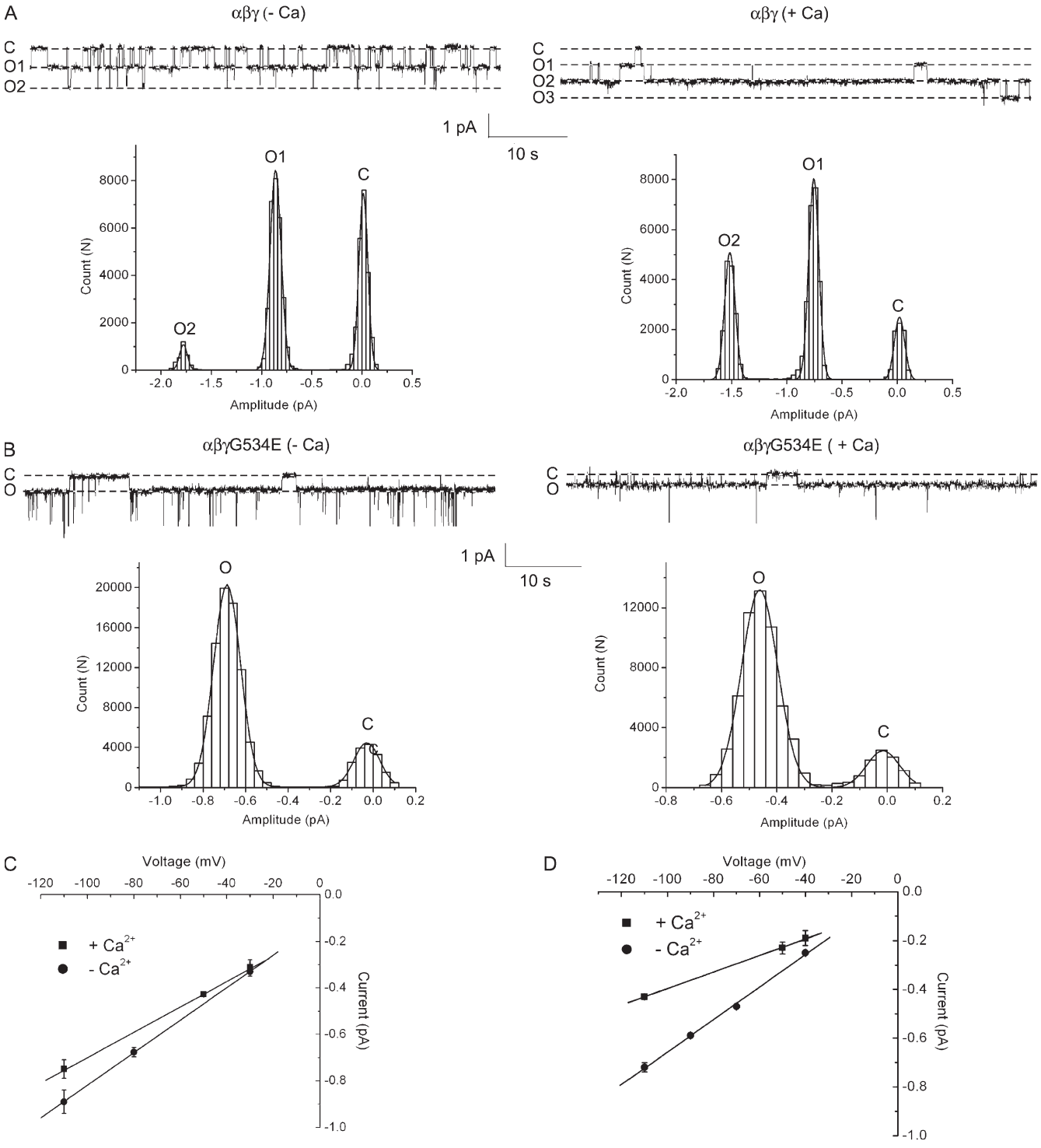

Figure 7. Single-channel properties of wt and αβγG534E channels. (A) Exemplar recordings taken from oocytes expressing wt channels with Li^+ as the permeant ion, in the presence (+Ca) or absence (−Ca) of 2 mM Ca^{2+} in the pipet as indicated. In each case, all-points histograms were constructed from ∼10-s regions of the trace above. The histograms were fit by three Gaussian functions corresponding to one closed and two open (O) levels as indicated. No subconductance levels were observed. (B) Exemplar recordings taken from oocytes expressing αβγG534E channels with Li^+ as the permeant ion, in the presence (+Ca) or absence (−Ca) of 2 mM Ca^{2+} in the pipet as indicated. Brief, large-amplitude transitions were noted during the recordings. We believe these are unlikely to represent ENaC and were ignored in the data analysis. For each trace, all-points histograms were constructed (from ∼10-s regions of recording) and fit by two Gaussian functions. No subconductance levels were observed. (C) Single-channel i-V relationship of wt channels with (+Ca) and without (−Ca) 2 mM Ca^{2+} in the pipet. The g_{Li} of wt channels with Ca^{2+} was 5.5 ± 0.2 pS and without Ca^{2+} was 7.0 ± 0.1 pS. (D) The single-channel conductance (g_{Li}) of αβγG534E channels with Ca^{2+} was 3.4 ± 0.1 pS and without Ca^{2+} was 6.7 ± 0.1 pS.

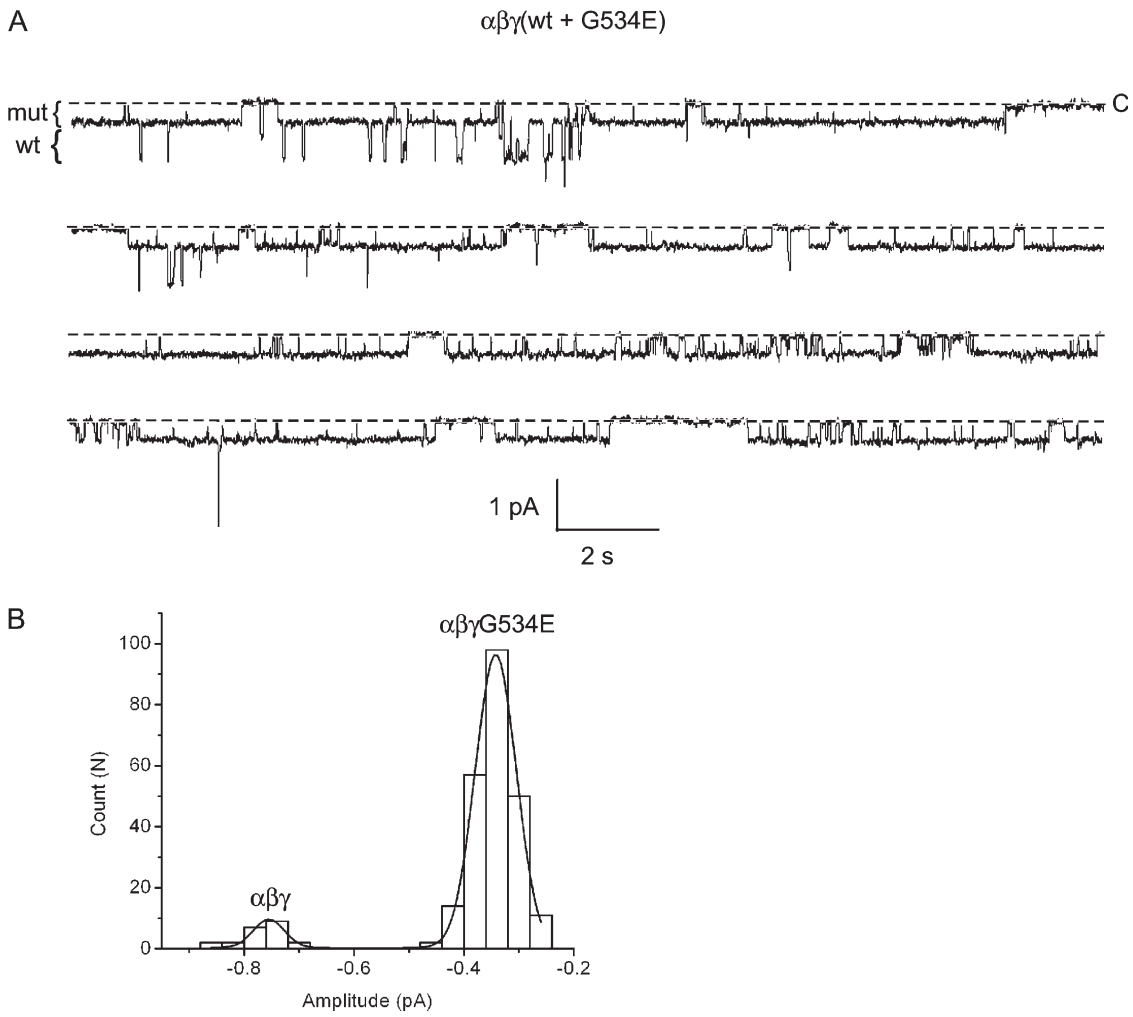

Figure 8. Coexpression of wt and mutant γG534E subunits. Oocytes were injected with γ-wt and γG534E subunits, together with wt α and β. (A) A continuous 80-s segment of a longer recording from a patch containing wt and mutant channels is shown. The pipet contained 110 mM Li^+ and 2 mM Ca^{2+}. The pipet voltage was 110 mV. The amplitude of wt and mutant conductance levels are indicated by brackets to the left of the trace. (B) An event-amplitude histogram was constructed by measuring the size of every open level transition for the full duration of the recording shown in A. The histogram was fit by two Gaussian functions with parameters (mean ± SD): 0.34 ± 0.04 and 0.76 ± 0.03 pA, corresponding to the mutant and wt conductance levels. Analysis of six other patches gave similar results.

from oocytes in which mutant subunits were mixed at an equimolar ratio, event-amplitudes corresponding to the larger αS592T conductance and the smaller αS589D conductance were observed, along with a novel intermediate conductance, not previously observed when either of the mutant channels was expressed alone in oocytes (Fig. 11 A). As done for all previous recordings, an event-amplitude histogram was constructed from the full duration of the record (~22 min in total). It was best fit by the sum of three Gaussian functions corresponding to the conductance level of αS589D channel, the αS592T channel, and an intermediate conductance most likely belonging to a αS589D/αS592T hybrid channel (Fig. 11 B). As is apparent in the segment of the record shown, the kinetics of the hybrid channel strongly resembled that of the αS589D channel, where open durations were on the scale of tens of milliseconds rather than hundreds or thousands of milliseconds as was typical for the αS592T channel. This shows that hybrid channels can be observed even for mutations that alter channel kinetics as well as conductance.

DISCUSSION

The main conclusion from this study is that epithelial Na^+ channels are composed of two α-, one β-, and one γ-subunit, consistent with previous findings (Firsov et al., 1998; Kosari et al., 1998; Dijkink et al., 2002). In this respect, ENaC subunit organization is similar to the fourfold subunit stoichiometry of K_{ir} and K_v channels and to the fourfold internally repeating structure of voltage-gated Na^+ and Ca^{2+} channels.

The use of unitary conductances to evaluate subunit stoichiometry was first employed by Veatch and Stryer (1977)

TABLE II

Summary of Coexpression Experiments

Subunits expressed (+αβγ)	Recordings (#)	Recordings with hybrids (#)	Channels counted		Time (s)
			wt	mutant	
αS589D	6	3	14	5	2,200
αS592T	4	2	8	6	730
βG529A	7	0	21	15	1,290
γG534E	7	0	15	11	1,670
αS589D, αS592T	3	1	11	3	2,810

The total number of recordings and the number of recordings in which hybrid conductances were measured are indicated. The number of wt or mutant channels observed (measured by counting the number of current level transitions belonging to one group or the other) is indicated. The total time was determined by summing the duration of individual recordings.

to demonstrate that gramicidin channels are dimers. This method was further exploited by Durkin and colleagues to show that mixtures of gramicidin monomers that were unmodified with those that contained single amino acid substitutions resulted in the formation of hybrid channels whose functional properties fell between those of the respective pure channel types (Durkin et al., 1990). As a means to estimate subunit stoichiometry of mammalian channel types, it has been employed before with success in the case of the nicotinic acetylcholine (nACh) receptor (Cooper et al., 1991), NMDA receptor (Premkumar and Auerbach, 1997), and CNG channel (Liu, et al., 1996). More recently, the appearance of single-channel currents intermediate in amplitude to those of pure TRPM6 and TRPM7 channels in coexpression studies has been used as evidence that complexes of subunits belonging to each channel type can occur (Li et al., 2006).

The rationale behind our experiments was very similar to those in the studies cited above. First, mutations were made in a single subunit at a time, so that the properties of the channel were altered. Subsequent coexpression of wt and mutant subunits resulted in the appearance of channels whose single-channel conductance fell between those of wt and mutant channels, but only in the case of the α-subunit. Since only a single intermediate conductance was observed, we estimated the number of α subunits in a channel to be two. Because no hybrid conductances were observed with either the β- or γ-subunit mixtures we deduced that a functional channel contains only one of each in a functional channel.

Our method relies on several assumptions. First, we had to assume that the wt and mutant channels used in this study did not have subconductances. The validity of this assumption is supported by the fact that multiple long recordings were taken from oocytes expressing these channels without subconductances being observed (or being observed only rarely). In the few cases when subconductances did appear, it seemed to be an oocyte batch-specific phenomenon rather than a property intrinsic to the channel being studied. With this criteria we excluded data from 2 out of >30 batches of oocytes used in our experiments. Wild-type and/or mutant recordings were taken from every batch of oocytes in which events intermediate to wt and mutant amplitudes were observed to ensure that the occurrence of a subconductance level was not falsely taken to be a hybrid channel event.

Second, we had to assume that that a hybrid conductance will lie between that of either "parent" conductance. There is good reason to suppose that it does. Subunit identity can influence conductance via either electrostatic effects on the permeating ion, or through steric effects, which alter pore geometry (Liu et al., 1996; Hille, 2001). In the case of the αS589Dβγ mutant, conductance is likely to be altered through an increase in the diameter of the pore of the channel. In a series of experiments, Kellenberger and colleagues showed that introduction of larger residues at this position increases the conductance of larger ions such as K^+ and NH_4^+ relative to that of smaller ions such as Li^+ and Na^+ (Kellenberger et al., 1999a, 2001). This was interpreted by assuming that the structure of the selectivity filter of ENaC is similar to K_{ir} or K_v channels, and that bulkier groups at this position widen the channel in such a way that the energetic cost of dehydrating the permeating ion is not adequately compensated for by interactions between the ion and the pore carbonyl oxygens. Thus, if the pore of ENaC is lined by two α subunits, it is likely that the effects of mutations in each would be additive.

Mutations at position 529 in the β-subunit, also in the putative selectivity filter (Fig. 1), are believed to alter single-channel conductance via a similar mechanism (Kellenberger et al., 1999b, 2001). Here, a glycine residue was changed to a bulkier alanine, with the effect of enlarging the pore. Coexpression of wt and mutant subunits resulted in only two types of conductances, a larger one corresponding to a wt channel and a smaller one corresponding to a mutant channel. Following the same logic as above, we interpreted the absence of an intermediate or hybrid conductance in this case to mean that there was only one β-subunit in a channel.

Introducing a charge at residue 534 of the γ-subunit (as in the G→E mutant), or homologous residues in the

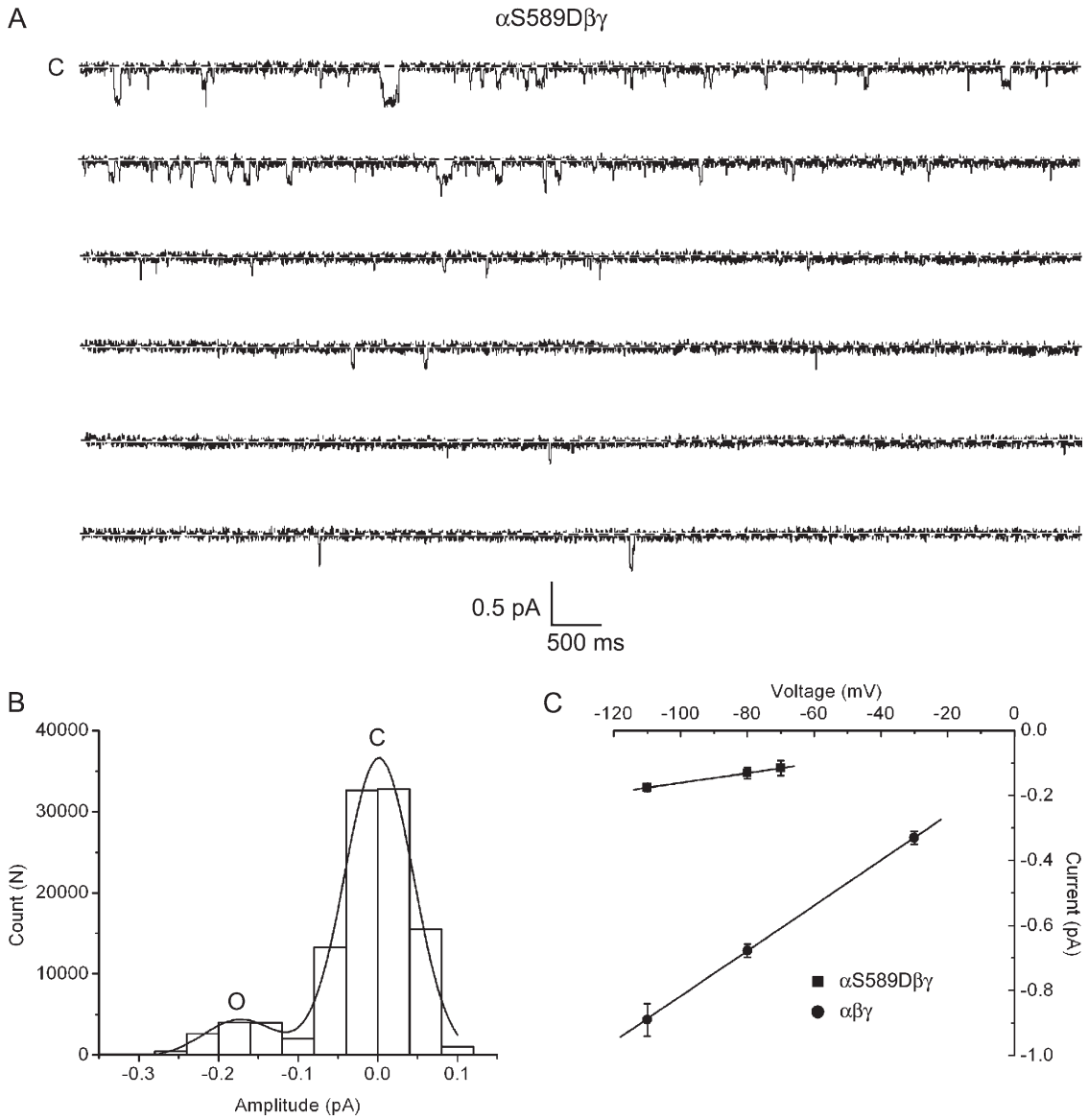

Figure 9. Single-channel properties of αS589Dβγ channels. Cell-attached patch recordings were taken from oocytes expressing αS589Dβγ channels. (A) An exemplar single-channel recording 60 s in duration from a patch containing an αS589Dβγ mutant. The pipet contained Li^+ as the charge carrier and the pipet voltage was +110 mV. (B) An all-points histogram was constructed from the single-channel recording obtained in A. The histogram was fit by two Gaussian functions corresponding to a single closed and open conductance level. (C) The slope conductance of αS589Dβγ channels was obtained from the single-channel i-V relationship. Conductance was calculated to be 1.9 ± 0.1 pS for the mutant channel compared with 7.0 ± 0.1 pS for the wt channel.

α or β subunits, decreases single-channel conductance in a Ca^{2+}-dependent manner (Schild et al., 1997). The effect of Ca^{2+} presumably arises from a fast channel block where the transition between open and closed states is so fast that conductance appears lowered. Moreover, it is believed that the Ca^{2+} ions interact with negatively charged glutamic acid residues, supporting the idea that the charged group faces the permeation pathway. Therefore, the reduction in Li^+ conductance observed in the αβγG534E channel when Ca^{2+} ions are present is caused by competition for the permeation pathway. As more charges are added (i.e., as more γG534E subunits are added), this competitive effect would be expected to increase in an additive manner. However, only two types of conductances were observed when wt and mutant γ subunits were coexpressed, a large conductance corresponding to a wt channel and smaller one corresponding to a mutant channel. Because intermediate conductances were never noted, we concluded that this was because only one γ-subunit is necessary for functional channel activity.

With the αS592Tβγ mutant, the mechanism by which single-channel conductance is increased is unclear without knowing more about the structure of the pore.

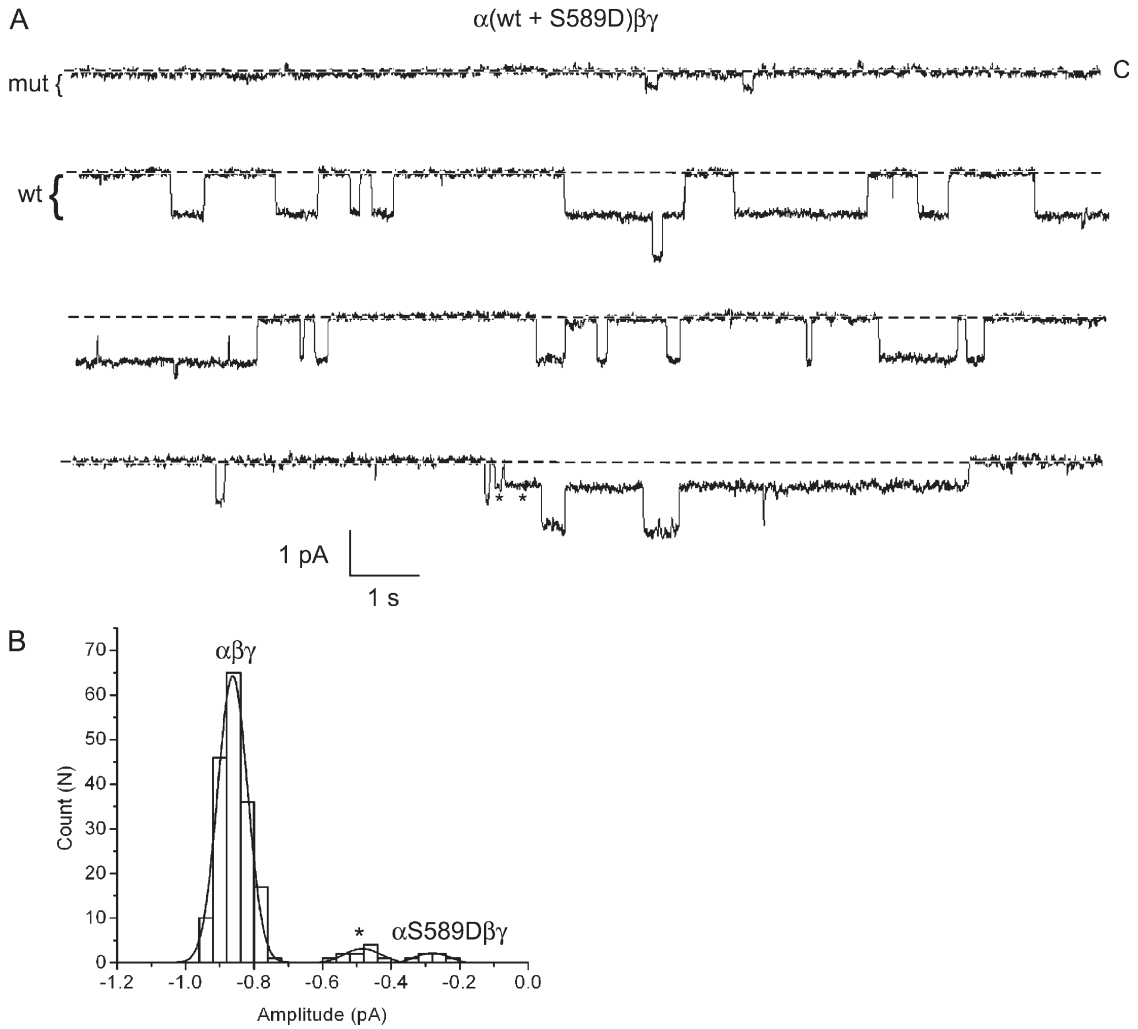

Figure 10. Coexpression of wt and mutant αS589D subunits. Oocytes were injected with α-wt and αS589D subunits, together with wt β and γ. (A) Four, 15-s segments of a longer recording containing mutant, wt, and hybrid channels in the patch are shown. Li^+ was the charge carrier, and the pipet voltage was 110 mV. The brackets to the left of the traces indicate the approximate amplitude of the wt and mutant channels. Stars denote openings that correspond to a hybrid conductance. (B) An event-amplitude histogram was constructed from this recording and was fit by three Gaussian functions with parameters (mean ± SD): 0.28 ± 0.06, 0.86 ± 0.04, and 0.48 ± 0.05 pA, corresponding to the mutant, wt, and hybrid conductance levels, respectively.

Irrespective of precisely how it occurs, permeation of Na^+ is enhanced. Again, the fact that we were able to record conductances intermediate to wt and mutant channels led us to the conclusion that at least one α-wt and one αS592T subunit could be present in a functional channel. As a final test of the reliability of our method, the two α mutants used in the study were also mixed and coinjected in oocytes. Once again, conductance levels corresponding to the smaller (αS589Dβγ) and larger (αS592Tβγ) channel were observed, in addition to an intermediate conductance, although in this case it arises from the coming together of two mutant α subunits.

Another assumption we had to make was that the kinetic behavior of the hybrid was reasonably similar to either the fully wt or fully mutant parent channel. It is a limitation of this approach that if hybrid events occurred extremely infrequently or exhibited flickery behavior that could not be resolved, they would not be counted.

The single-channel data presented in this study imply that there is only one β- and one γ-subunit in the functional channel complex. They also demonstrate that there are at least two α subunits/channel. Although we did not observe evidence for more than two α's/channel (i.e., more than one hybrid conductance), this possibility cannot entirely be ruled out. This is partly because the differences in the amplitudes of hybrid and fully mutant or fully wt openings are only in the range of tenths of a picoampere, and it is therefore conceivable that two or more intermediate conductances might not be resolved in the histograms. However, the fact that the standard deviations (widths) of the Gaussians corresponding to the hybrid conductance were roughly

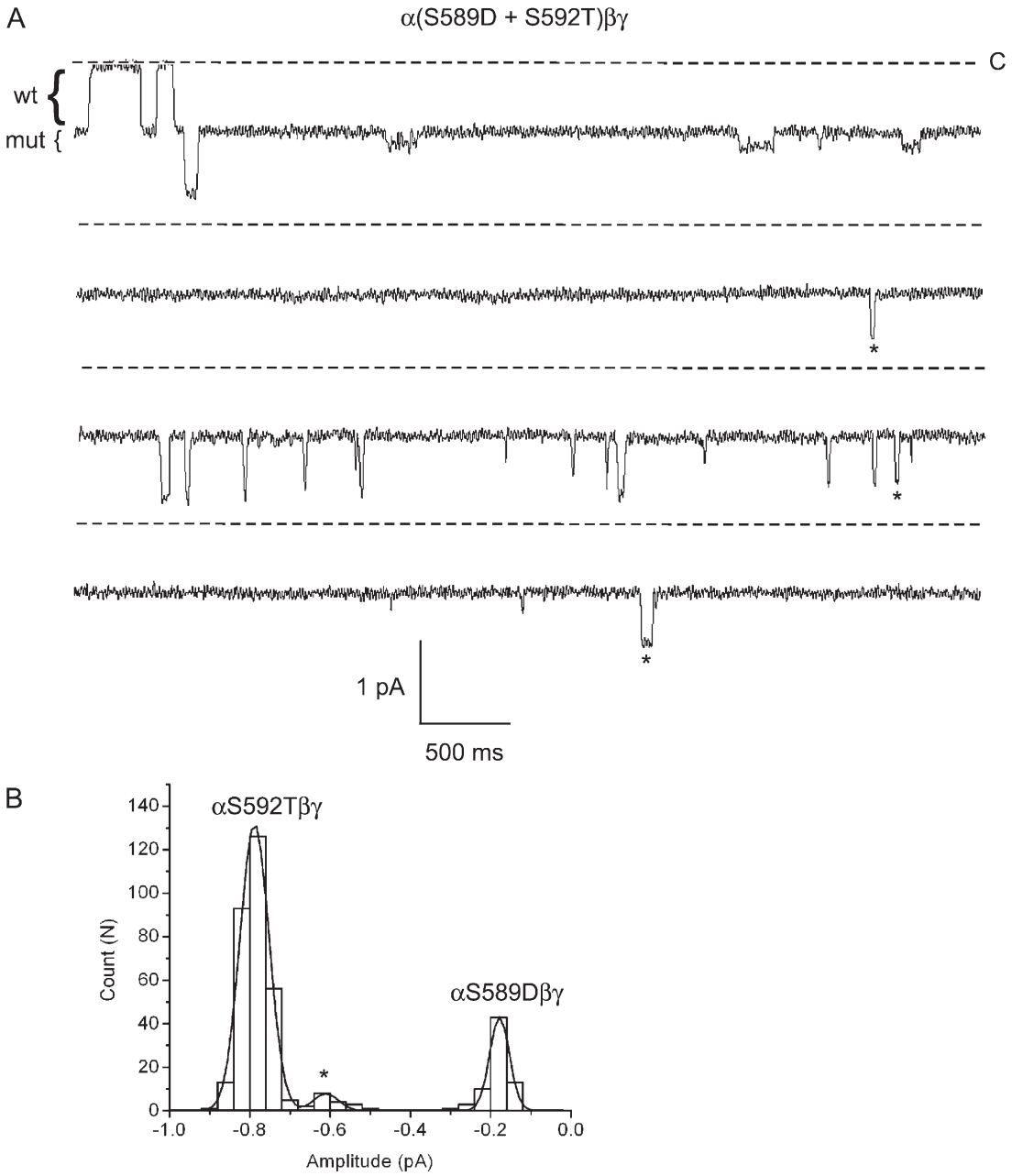

Figure 11. Coexpression of mutant αS589D and αS592T subunits. Oocytes were injected with αS589D and αS592T subunits, together with wt β and γ. (A) Four, 5-s segments of a longer recording containing mutant, wt, and hybrid channels in the patch are shown. The brackets to the left of the traces indicate the approximate amplitudes of wt and mutant channels. Li^+ was the charge carrier, and the pipet voltage was 110 mV. Stars denote openings of a hybrid channel. (B) An event-amplitude histogram was constructed from this recording and was fit by three Gaussian functions with parameters (mean ± SD): 0.18 ± 0.03, 0.79 ± 0.04, and 0.61 ± 0.03 pA, corresponding to the αS589D, αS592T, and hybrid conductance levels, respectively.

the same as those corresponding to wt and mutant conductances renders this possibility less likely.

Previous attempts to assess subunit stoichiometry using functional assays have themselves made assumptions that were not required in this study. For instance, it was not necessary to our analysis that the subunits used had an equal probability of expression and coassembly. This assumption was fundamental to the validity of studies in oocytes where the sensitivity of expressed Na^+ current to blockers or toxins was used to determine the number of subunits in a functional channel (Firsov et al., 1998; Kosari et al., 1998; Snyder et al., 1998). These approaches also depended on channel gating in mutants or hybrids being similar to wt channels. In coexpression experiments, the number of distinct current level transitions or conductances (reflecting channels in the patch) counted belonging to either wt or mutant channels was roughly the same when changes were made at αS592,

βG529, or γG534 (8 wt, 6 mutant for αS592T; 21 wt, 15 mutant for βG529A; 15 wt, 11 mutant for γG534E). This suggests that there was unlikely to be much of a difference in wt and mutant subunit expression levels in these instances. On the other hand, in experiments where the αS589D subunit was mixed with wt subunits, only 5 of the 19 conductances counted in six recordings corresponded to the known magnitude of a fully mutant channel. It was unclear to us whether the low number of conductances counted was due to an expression level difference or was related to channel gating. However, these coexpression experiments demonstrate that hybrid events may still be observed even if mutant subunit expression is reduced and the kinetics of mutant channels are different from wt channels.

The single-channel method also has some advantages over other approaches that have been used to investigate subunit stoichiometry. For instance, biochemical studies that use sucrose density centrifugation to determine stoichiometry have produced data that support both a 2α:1β:1γ (Dijkink et al., 2002) and 3α:3β:3γ subunit order (Snyder et al., 1998). However, these methods rely on a parameter (mass) that may not reflect the composition of a functional unit at the membrane surface. Another possibility to consider is that proteins that help in the assembly or folding of ENaC are captured in these assays, contributing to a larger mass of the channel complex in these studies. Alternatively, it is also possible in extracting ENaC protein from cells with detergents, subunits may dissociate, thereby reducing the perceived size of the channel complex. Potential aggregation of channel subunits, both with each other and ancillary proteins is also an issue in the use of freeze-fracture images to determine the number of subunits comprising a channel, leading to an overestimation of subunits (eight or nine) per channel in this case (Eskandari et al., 1999).

The optical techniques of fluorescence-resonance energy transfer (FRET) and total internal reflection fluorescence (TIRF) have produced data supporting a "higher-order" subunit stoichiometry (Staruschenko et al., 2004, 2005), more consistent with the nonomeric channel proposed by Snyder and colleagues (Snyder et al., 1998; Eskandari et al., 1999) than the competing tetrameric model (Firsov et al., 1998; Kosari et al., 1998; Dijkink et al., 2002). However, FRET may not distinguish between inter- and intrachannel subunit FRET in the event channels are clustered at the membrane. Thus, the FRET measured between two β or two γ subunits might reflect aggregates of tetrameric functional units. It is possible, although in our view unlikely, that the channel consists of greater than one β- or γ-subunit, but that only a single copy of each subunit contributes to the channel pore. Our measurements would then only count subunits lining the pore and not additional subunits that may still contribute to the overall channel structure. However, it should be noted that in the original experiments performed suggesting the higher-order stoichiometry, the assumption was that all the subunits contribute to the ion permeation pathway (Snyder et al., 1998).

Using single-channel currents to study subunit stoichiometry, by definition, restricts measurements to functional channels present at the membrane surface. In addition, the presence of several channels in the patch, though not ideal, does not seriously affect the analysis. It should be noted, however, that as with any study that contends with the issue of ENaC structure, the relevance of our oocyte data to the epithelial cell is an open question. The idea of a fixed subunit stoichiometry is appealing, but several lines of evidence suggest that this does not have to be the case. Distinct responses of ENaC subunit mRNA and protein to changes in aldosterone levels, K^+ or Na^+ depletion, and water restriction have been noted in several studies (for review see Weisz and Johnson, 2003). Moreover, there is evidence that channels composed of multimers of just two subunits can form in both heterologous expression systems and in epithelial cells (Fyfe and Canessa, 1998; Weisz and Johnson, 2003). Presumably, there is at least some possibility of forming such channels even when all three subunits are present.

To recapitulate, we have used a single-channel approach to determine the subunit stoichiometry of ENaC. Our results are consistent with a tetrameric subunit stoichiometry for ENaC similar to many previously described K^+, Na^+, and Ca^{2+} selective channels.

We thank David Finkelstein for technical assistance and Olaf S. Andersen, Johan Edvinsson, Yuyang Zhang, and Gustavo Frindt for helpful discussions.

This work was supported by National Institutes of Health grant DK59659.

Erik Hviid Larsen served as guest editor.

Submitted: 11 December 2006
Accepted: 25 May 2007

REFERENCES

Anantharam, A., Y. Tian, and L.G. Palmer. 2006. Open probability of the epithelial sodium channel is regulated by intracellular sodium. *J. Physiol.* 574.2:333–347.

Benos, D.J., and B.A. Stanton. 1999. Functional domains within the degenerin/epithelial sodium channel (Deg/ENaC) superfamily of ion channels. *J. Physiol.* 520.3:631–644.

Canessa, C.M., L. Schild, G. Buell, B. Thorens, I. Gautschi, J.D. Horisberger, and B.C. Rossier. 1994. Amiloride-sensitive epithelial Na^+ channel is made of 3 homologous subunits. *Nature.* 367:463–467.

Cooper, E., S. Couturier, and M. Ballivet. 1991. Pentameric structure and subunit stoichiometry of a neuronal nicotinic acetylcholine-receptor. *Nature.* 350:235–238.

Dijkink, L., A. Hartog, C.H. van Os, and R.J.M. Bindels. 2002. The epithelial sodium channel (ENaC) is intracellularly located as a tetrAm. *Pflugers Arch.* 444:549–555.

Durkin, J.T., R.E. Koeppe II, and O.S. Andersen. 1990. Energetics of gramicidin hybrid channel formation as a test for structural equivalence. Side-chain substitutions in the native sequence. *J. Mol. Biol.* 211:221–234.

Eskandari, S., P.M. Snyder, M. Kreman, G.A. Zampighi, M.J. Welsh, and E.M. Wright. 1999. Number of subunits comprising the epithelial sodium channel. *J. Biol. Chem.* 274:27281–27286.

Firsov, D., I. Gautschi, A.M. Merillat, B.C. Rossier, and L. Schild. 1998. The heterotetrameric architecture of the epithelial sodium channel (ENaC). *EMBO J.* 17:344–352.

Fyfe, G.K., and C.M. Canessa. 1998. Subunit composition determines the single channel kinetics of the epithelial sodium channel. *J. Gen. Physiol.* 112:423–432.

Hansson, J.H., C. Nelsonwilliams, H. Suzuki, L. Schild, R. Shimkets, Y. Lu, C. Canessa, T. Iwasaki, B. Rossier, and R.P. Lifton. 1995. Hypertension caused by a truncated epithelial sodium channel γ-subunit: genetic heterogeneity of Liddle syndrome. *Nat. Genet.* 11:76–82.

Hille, B. 2001. Ionic Channels of Excitable Membranes. Third edition. Sinauer Associates, Inc., Sunderland, MA. 814 pp.

Kellenberger, S., I. Gautschi, and L. Schild. 1999a. A single point mutation in the pore region of the epithelial Na^+ channel changes ion selectivity by modifying molecular sieving. *Proc. Natl. Acad. Sci. USA.* 96:4170–4175.

Kellenberger, S., N. Hoffmann-Pochon, I. Gautschi, E. Schneeberger, and L. Schild. 1999b. On the molecular basis of ion permeation in the epithelial Na^+ channel. *J. Gen. Physiol.* 114:13–30.

Kellenberger, S., M. Auberson, I. Gautschi, E. Schneeberger, and L. Schild. 2001. Permeability properties of ENaC selectivity filter mutants. *J. Gen. Physiol.* 118:679–692.

Kellenberger, S., and L. Schild. 2002. Epithelial sodium channel/degenerin family of ion channels: a variety of functions for a shared structure. *Physiol. Rev.* 82:735–767.

Kellenberger, S., I. Gautschi, and L. Schild. 2003. Mutations in the epithelial Na^+ channel ENaC outer pore disrupt amiloride block by increasing its dissociation rate. *Mol. Pharmacol.* 64:848–856.

Kosari, F., S.H. Sheng, J.Q. Li, D.O.D. Mak, J.K. Foskett, and T.R. Kleyman. 1998. Subunit stoichiometry of the epithelial sodium channel. *J. Biol. Chem.* 273:13469–13474.

Li, M., J. Jiang, and L. Yue. 2006. Functional characterization of homo- and heteromeric channel kinases TRPM6 and TRPM7. *J. Gen. Physiol.* 127:525–537.

Liu, D.T., G.R. Tibbs, and S.A. Siegelbaum. 1996. Subunit stoichiometry of cyclic nucleotide-gated channels and effects of subunit order on channel function. *Neuron.* 16:983–990.

Mackinnon, R. 1991. Determination of the subunit stoichiometry of a voltage-activated potassium channel. *Nature.* 350:232–235.

Palmer, L.G., and G. Frindt. 1986. Amiloride-sensitive Na channels from the apical membrane of the rat cortical collecting tubule. *Proc. Natl. Acad. Sci. USA.* 83:2767–2770.

Palmer, L.G., and O.S. Andersen. 1989. Interactions of amiloride and small mono-valent cations with the epithelial sodium channel: inferences about the nature of the channel pore. *Biophys. J.* 55:779–787.

Premkumar, L.S., and A. Auerbach. 1997. Stoichiometry of recombinant *N*-methyl-D-aspartate receptor channels inferred from single-channel current pattern. *J. Gen. Physiol.* 110:485–502.

Schild, L., Y. Lu, I. Gautschi, E. Schneeberger, R.P. Lifton, and B.C. Rossier. 1996. Identification of a PY motif in the epithelial Na channel subunits as a target sequence for mutations causing channel activation found in Liddle's syndrome. *EMBO J.* 15:2381–2387.

Schild, L., E. Schneeberger, I. Gautschi, and D. Firsov. 1997. Identification of amino acid residues in the α, β, and γ subunits of the epithelial sodium channel (ENaC) involved in amiloride block and ion permeation. *J. Gen. Physiol.* 109:15–26.

Shimkets, R.A., D.G. Warnock, C.M. Bositis, C. Nelsonwilliams, J.H. Hansson, M. Schambelan, J.R. Gill, S. Ulick, R.V. Milora, J.W. Findling, et al. 1994. Liddles syndrome: heritable human hypertension caused by mutations in the β-subunit of the epithelial sodium channel. *Cell.* 79:407–414.

Snyder, P.M., M.P. Price, F.J. Mcdonald, C.M. Adams, K.A. Volk, B.G. Zeiher, J.B. Stokes, and M.J. Welsh. 1995. Mechanism by which Liddles syndrome mutations increase activity of a human epithelial Na^+ channel. *Cell.* 83:969–978.

Snyder, P.M., C. Cheng, L.S. Prince, J.C. Rogers, and M.J. Welsh. 1998. Electrophysiological and biochemical evidence that DEG/ENaC cation channels are composed of nine subunits. *J. Biol. Chem.* 273:681–684.

Snyder, P.M. 2002. The epithelial Na^+ channel: cell surface insertion and retrieval in Na^+ homeostasis and hypertension. *Endocr. Rev.* 23:258–275.

Staruschenko, A., J.L. Medina, P. Patel, M.S. Shapiro, R.E. Booth, and J.D. Stockand. 2004. Fluorescence resonance energy transfer analysis of subunit stoichiometry of the epithelial Na^+ channel. *J. Biol. Chem.* 279:27729–27734.

Staruschenko, A., E. Adams, R.E. Booth, and J.D. Stockand. 2005. Epithelial Na^+ channel subunit stoichiometry. *Biophys. J.* 88:3966–3975.

Veatch, W., and L. Stryer. 1977. The dimeric nature of the gramicidin A transmembrane channel: conductance and fluorescence energy transfer studies of hybrid channels. *J. Mol. Biol.* 113:89–102.

Waldmann, R., G. Champigny, and M. Lazdunski. 1995. Functional degenerin-containing chimeras identify residues essential for amiloride-sensitive Na^+ channel function. *J. Biol. Chem.* 270:11735–11737.

Weisz, O.A., and J.P. Johnson. 2003. Noncoordinate regulation of ENaC: paradigm lost? *Am. J. Physiol. Renal Physiol.* 285:F833–F842.